Title:

Acute Toxicity of Major Geochemical Ions to Fathead Minnows (*Pimephales promelas*). Part B: Modeling Ion Toxicity

Authors:

Russell J. Erickson[1]

David R. Mount[1]

Terry L. Highland[1]

J. Russell Hockett[1]

Dale J. Hoff[1]

Correne T. Jenson[1]

Teresa J. Norberg-King[1]

Brandy Forsman[1]

[1]U.S. Environmental Protection Agency

Office of Research and Development

Center for Computational Toxicology and Ecology

Great Lakes Toxicology and Ecology Division

6201 Congdon Blvd, Duluth, MN 55804 USA

Corresponding author:

Russell J. Erickson

erickson.russell@epa.gov

Acknowledgments:

The authors wish to thank Kevin Lott for supervising the culture of test organisms used in this research and to John Nichols, James Lazorchak, and N anonymous referees for helpful reviews.

Disclaimer:

The views expressed in the present article are those of the authors and do not necessarily reflect the views or policies of the U.S. Environmental Protection Agency. Mention of trade names or commercial products does not constitute endorsement or recommendation for use.

Data availability:

Data are available through the USEPA Environmental Dataset Gateway (https://edg.epa.gov/metadata/catalog/main/home.page) or by request from the corresponding author (erickson.russell@epa.gov).

TITLE: Acute Toxicity of Major Geochemical Ions to Fathead Minnows (*Pimephales promelas*). Part B: Modeling Ion Toxicity

RUNNING HEAD: Modeling Major Ion Toxicity to Fathead Minnow

ABSTRACT: This paper reports on mathematical models for the acute LC50s of major geochemical ions (Na^+, K^+, Ca^{2+}, Mg^{2+}, Cl^-, SO_4^{2-}, HCO_3^-/CO_3^{2-}) to fathead minnows (*Pimephales promelas*), based on an extensive series of experiments presented in a companion paper. Toxicity relationships across different dilution waters, individual salts, and salt mixtures suggest six independent mechanisms of toxicity to consider in modeling efforts, including Mg/Ca-specific toxicity, osmolarity-related toxicity, SO_4-specific toxicity, K-specific toxicity, effects of high pH/alkalinity, and a multiple ion-related toxicity at low Ca distinct from the other mechanisms. Models are evaluated using chemical activity-based exposure metrics pertinent to each mechanism, but concentration-based alternative models that are simpler to apply are also addressed. These models are compared to those previously provided for *Ceriodaphnia dubia*, and various issues regarding their application to risk assessments are discussed.

KEY WORDS: Aquatic Toxicology, Major Geochemical Ions, *Pimephales promelas*, Fathead Minnow, Toxicity Mechanisms, Mixture Toxicity, Mathematical Models

INTRODUCTION

The impact on aquatic communities of anthropogenic inputs of major geochemical ions (Na^+, K^+, Ca^{2+}, Mg^{2+}, Cl^-, SO_4^{2-}, and HCO_3^-/CO_3^{2-}) are of considerable concern (see reviews by Hintz and Relyea, 2019; Cañedo-Argüelles et al., 2019; Berger et al. 2019; Schuler et al., 2019; Cañedo-Argüelles, 2020; Kaushal et al., 2021). Such exposures inherently involve complex mixtures, involving not only the individual ions but also their various chemical complexes. The relative concentrations of these chemical species can vary widely, thereby causing toxicities to vary, and warranting risk assessment methods that address such variation. A companion paper (Erickson et al., 2022) reports on 170 acute toxicity tests with fathead minnow (*Pimephales promelas*) that evaluated 1) the impact of test water characteristics on the toxicity of individual major ion salts and 2) toxicity interactions in binary mixtures of salts in a single test water (amended Lake Superior water, ALSW; Mount et al., 2016). The present paper develops mathematical models for the observed LC50s.

Erickson et al. (2022) identified six apparent mechanisms of toxicity to be considered in modeling the acute toxicity of major ion mixtures to fathead minnows.

Mg/Ca-related toxicity. The toxicities of Mg and Ca salts and their mixtures are generally related to the chemical activities of the cations and are concentration additive, indicating a common mechanism of toxicity. The potency of Mg for this mechanism also decreases with increasing Ca. However, $MgCO_3$-dominated exposures indicate separate effects of high pH/alkalinity beyond that from Mg.

Osmolarity-related toxicity. At $\{Ca\} \approx 0.3$mM and above (braces {} denote chemical activity), LC50s for NaCl and Na_2SO_4 have osmolarities similar to that for mannitol, and also to internal osmolarities reported for teleost fish. In ALSW, NaCl and mannitol toxicities are also

largely additive, further suggesting a shared mechanism related to osmotic effects. However, at lower Ca, Na salt toxicities increase while mannitol toxicity remains constant, suggesting osmolarity per se is not related to ion toxicity at lower Ca.

SO_4-related toxicity at lower Ca. At {Ca} < 0.3mM, LC50s for NaCl and Na_2SO_4 diverge not only from mannitol but from each other. The greater toxicity of Na_2SO_4, as well as interactions in binary salt mixtures including SO_4, indicate a Ca-dependent, SO_4-driven toxicity when it is the dominant anion.

Multi-ion toxicity at lower Ca. Interactions across binary salt mixtures suggest that the toxicity associated with NaCl at lower Ca is not solely Na-driven but rather involves multiple ions; however, the specific ions contributing to this toxicity and their relative potencies are uncertain.

High pH/alkalinity-related toxicity. Toxicities of exposures dominated by $MgCO_3$ or $NaHCO_3$ to fathead minnow are greater than their respective Cl salts, apparently related to effects of combined high pH (>9) and alkalinity ({HCO_3}>15 meq/L) in addition to, or instead of, other ions. There are insufficient data to address how this toxicity varies with pH, alkalinity, and other ions.

K-related toxicity. Toxicities of K salts to fathead minnow are attributable to the cation and are largely independent of the toxicities of other salts, except for contributing to mechanisms involving all ions. In contrast to *Ceriodaphnia dubia* (Mount et al. 2016), the potency of K to fathead minnows is not affected by Na, but is reduced by increasing all ions in dilution water; however, the specific cause of this is not clear.

The present paper addresses development of models for the first four of these mechanisms. To simplify the presentation, the paper is organized around these four

mechanisms rather than the traditional Methods/Results/Discussion format. For each mechanism, we present the pertinent data from the companion paper and discuss attributes relevant to modeling. We then evaluate models that use chemical activity-based exposure metrics, due to the importance of activity in determining toxic response (Erickson et al. 2017, 2018, 2022). Because the computational complexity of activity-based exposure metrics can make their application more difficult and because appropriate activity-based metrics are sometimes uncertain, we also evaluate models that use concentration-based exposure metrics. For high pH/alkalinity and K related mechanisms, for which available data do not support model development, screening values are identified to use in conjunction with the models for the other mechanisms. The mechanics of model application are demonstrated using data from the literature, and issues regarding scope of model applicability and alternative exposure metrics for further model development are discussed.

MAGNESIUM/CALCIUM-RELATED TOXICITY

Data for model development

Figure 1A provides all 96-h LC50s from Erickson et al. (2022) for the acute toxicity to fathead minnow of individual Mg and Ca salts, Mg×Mg salt mixtures, and Mg×Ca salt mixtures, plotted as {Mg} vs {Ca} at the LC50. The chemical activities are as calculated and reported by Erickson et al. (2022) using the chemical speciation program Visual Minteq (version 3.1, https://vminteq.lwr.kth.se/visual-minteq-ver-3-1).

In this and subsequent figures, the larger symbols denote data used in model development. In Figure 1A, these data show a tight correlation of toxicity to {Mg} and {Ca} that is consistent across $MgCl_2$, $MgSO_4$, $MgCl_2$×$MgSO_4$ mixtures, and Cl-dominated $MgCl_2$×$MgCO_3$ mixtures, with {Mg} at the LC50 first increasing as Ca increases and then decreasing as Ca

becomes high enough to significantly contribute to additive toxicity. There is, however, more data scatter at the lowest {Ca} than at other {Ca}.

The smaller symbols are to distinguish data used for model development from those attributable to other mechanisms or used to further help validate the mechanism. In Figure 1A, this includes $MgCO_3$-dominated exposures in which high pH/alkalinity apparently contributes to toxicity, so is not addressed by this Mg/Ca-related toxicity model. Also included are Mg and Ca gluconate LC50s, these chemicals being used to validate whether toxicity is related to Mg and Ca activities, but not included in model development.

Figure 1B provides the same data as Figure 1A, but on a concentration basis. This basis for expressing LC50s shows greater variability than for activity-based LC50s. In particular, LC50s for $MgCl_2$ and $MgSO_4$ differ, generally by about a factor of 2. This divergence is attributable to the complexation of Mg by SO_4, the formation of this less toxic complex reducing the toxicity of $MgSO_4$ relative to $MgCl_2$ on a concentration basis.

Model formulation.

Because of similar relationships for Mg/Ca toxicity, the modeling approach for fathead minnow is based on that used previously for *C. dubia* (Erickson et al., 2018). This model has two mathematical components: 1) the LC50 for Mg in the absence of other toxicity ($LC50_{MgOnly}$) as a function of Ca and 2) the additive toxicity of Ca and Mg. We will describe the formulation of the model on an activity basis, but this model structure also applies to the concentration-based model.

At {Ca} low enough to contribute negligible toxicity, the relationship of {Mg}-based LC50s to {Ca} is curved (Figure 1A). This is modeled using a hyperbolic equation for $\log_{10}LC50_{MgOnly}$ versus $\log_{10}\{Ca\}$:

$$\left(\log_{10} LC50_{MgOnly} - P_1\right) \times \left(\log_{10}\{Ca\} - P_2\right) = -P_3$$

$$\Rightarrow LC50_{MgOnly} = 10^{\left(P_1 - \frac{P_3}{\log_{10}\{Ca\} - P_2}\right)} \quad \text{(Eq. 1)}$$

where the parameter P_1 is an upper asymptote for $\log_{10}LC50_{MgOnly}$, P_2 is a lower asymptote for $\log_{10}\{Ca\}$, and P_3 is a shape parameter (sharpness/eccentricity) for the hyperbola. Estimates for these asymptotes are uncertain extrapolations beyond the limits of the data and do not have definite toxicological or physiological significance, and we don't assert this relationship is necessarily hyperbolic past the data limits. Rather, this model is simply intended to provide a good representation of the curvature within the range of the data. To avoid the uncertain estimation of P1, Erickson et al. (2018) replaced it in the *C. dubia* model with a parameter for $LC50_{MgOnly}$ within the range of the data; however, this modification resulted in a more complicated model that is not used here in the interest of simplifying model formulation and application.

The second component of the Mg/Ca toxicity model is a concentration-additive interaction of Mg and Ca toxicities, consistent with a common mechanism of toxicity:

$$1 = \frac{\{Mg\}_M}{LC50_{MgOnly}} + \frac{\{Ca\}_M}{LC50_{CaOnly}}$$

$$\Rightarrow \{Mg\}_M = LC50_{MgOnly} \times \left(1 - \frac{\{Ca\}_M}{LC50_{CaOnly}}\right) \quad \text{(Eq. 2)}$$

where $LC50_{CaOnly}$ is the LC50 for Ca in the absence of other toxicity and $\{Mg\}_M$ and $\{Ca\}_M$ denote {Mg} and {Ca} at the LC50 for a specified mixture "M".

By substituting the expression for $LC50_{MgOnly}$ from Equation 1 into Equation 2, the overall model for Mg/Ca-related toxicity is:

$$\{Mg\}_M = 10^{\left(P_1 - \frac{P_3}{\log_{10}\{Ca\}_M - P_2}\right)} \times \left(1 - \frac{\{Ca\}_M}{LC50_{CaOnly}}\right) \quad \text{(Eq. 3)}$$

Activity-based model parameterization and performance.

As further described in Erickson et al. (2018), model parameters were estimated by maximum likelihood analysis using custom software written with Intel Visual Fortran Compiler XE 2015 (Intel Corporation) and Winteracter 13.0 (Interactive Software Services Ltd.). The parameterized model equation for activity-based Mg/Ca toxicity, using mM activity units, is:

$$\{Mg\}_M = 10^{1.51 - \frac{0.68}{\log_{10}\{Ca\}_M + 2.51}} \times \left(1 - \frac{\{Ca\}_M}{15.1}\right) \quad \text{(Eq. 4)}$$

The model line in Figure 1A closely follows the data used for model parameterization, although the more variable LC50s at low {Ca} involve greater scatter from the model. The log residual standard deviation for this fitted model is 0.061 but is only 0.048 if the variable data at low Ca are not included. This is similar to the pooled inter-experimental log standard deviation of 0.044 calculated from the repeated tests in ALSW for $MgCl_2$, $MgSO_4$, and $CaCl_2$ in Figure 1A. This similarity indicates little lack of fit due to model error. The residual plot in Figure 1C affirms a good model fit, with LC50s falling within ± 2 of the inter-experimental log standard deviation except at the lowest Ca, and residuals showing no apparent trends with Ca.

The LC50s for $MgCO_3$-dominated exposures average ≈40% below the model (Figure 1A). If Mg dominated solutions with such extreme pH/alkalinity are an issue in a risk assessment, approaches that better address these circumstances should be used. The Mg gluconate LC50 also is moderately below the model and is 28% lower than its companion test with $MgCl_2$ (Erickson et al., 2022); however, this deviation includes uncertainty in the calculated complexation of Mg by gluconate, and is not large enough to be inconsistent with treating {Mg}

as the primary driving force for toxicity. The {Ca}-based LC50 for Ca gluconate is indeterminate because there was just 20% mortality at the highest test concentration of 13.1 mM (Erickson. et al., 2022). Based on the exposure-response slope in the companion test with $CaCl_2$, the {Ca}-based LC50 for Ca gluconate should be very close to that for the $CaCl_2$ test (15.8 mM; Erickson et al., 2022).

Concentration-based model parameterization and performance

The model based on Mg and Ca concentrations (Figure 1B) was also developed using Equation 3, simply switching from activity-based to concentration-based units for the variables and parameters. The resultant parameterized model, using mM concentration units, is:

$$[Mg]_M = 10^{\left(2.49 - \frac{1.58}{\log_{10}[Ca]_M + 2.28}\right)} \times \left(1 - \frac{[Ca]_M}{48.4}\right) \quad \text{(Eq. 5)}$$

The model line in Figure 1B strikes a compromise within the data variation, although for 1 mM < [Ca] < 10 mM it lies closer to the $MgSO_4$ data than the $MgCl_2$ data and lacks the flatness of the $MgCl_2$ LC50s. The overall residual log standard deviation is 0.112, much higher than for the activity-based model, and also higher than the pooled log standard deviation of 0.066 for concentration-based LC50s across repeated tests of $MgCl_2$, $MgSO_4$, and $CaCl_2$ in ALSW. Two residual log standard deviations correspond to a factor of 1.7 for this concentration-based model versus 1.25 for the activity-based model, and this standard deviation would be even higher if the tightly-spaced, Ca-driven LC50s were not included. The poorer model fit is clear in the residual plot (Figure 1D); even with a wider uncertainty band for the inter-experimental variation, data are more frequently outside the band and there are large disparities between the residuals for $MgCl_2$ and $MgSO_4$ at 0.3 mM < [Ca] < 10 mM.

This concentration-based model therefore is substantially inferior to the activity-based model. If it is impractical to apply the activity-based model, the concentration-based model should be applied cautiously, with recognition of the greater uncertainties and biases. An alternative approach for risk screening purposes might be to develop a concentration-based model from just the $MgCl_2$ data, which should result in an equation unlikely to underestimate toxicity.

Comparison to C. dubia

Figure 1A includes the activity-based Mg/Ca-related toxicity model for *C. dubia* from Erickson et al. (2018), to compare to that for fathead minnow. Although the relationships for the two species are similar regarding concentration additivity and the relative effects of Ca on Mg potency, their sensitivities are substantially different, with the activity-based *C. dubia* model indicating 2-3 times greater sensitivity than for fathead minnows. Besides this sensitivity difference, the only substantial difference between the two species is that the enhanced toxicity of $MgCO_3$-dominated exposures to fathead minnow was not observed for *C. dubia*. This might mean that fathead minnows are subject to a mechanism of toxicity to which *C. dubia* are less susceptible. However, because *C. dubia* is more sensitive to Mg than fathead minnow, it might simply mean that *C. dubia* succumbs to Mg before lethal conditions of high pH/alkalinity are reached.

The concentration-based *C. dubia* model from Erickson et al. (2018) is shown in Figure 1B. The offset in the concentration-based models for the two species is even larger (factor of 3 to 4) than for the activity-based models. This is because activity does not increase proportionately with concentration, due to more complexation and lower activity coefficients at higher concentrations. Like the fathead minnow model, the concentration-based *C. dubia*

model suffers from systematic discrepancies between $MgCl_2$ and $MgSO_4$ LC50s and larger uncertainties than the activity-based model (see Figure 6A in Erickson et al. 2018).

OSMOLARITY-RELATED TOXICITY

Data for model development

Figure 2A provides all LC50s from Erickson et al. (2022) for the acute toxicity to fathead minnow of individual Na salts (excluding $NaHCO_3$ tests with substantial Ca precipitation during the test), $CaCl_2$, mannitol, Na×Na salt mixtures, Na×Ca salt mixtures, and Na×mannitol mixtures, plotted as estimated osmolarity versus {Ca} at the LC50. The larger symbols denote data selected for use in developing a model for osmolarity-related toxicity, while the smaller symbols denote data to provide context for osmolarity-related toxicity relative to other mechanisms and to help explain data selection.

This data selection is based on evidence and arguments that certain exposures in Figure 4A involve osmolarity-related toxicity (Erickson et al., 2022). Osmolarity-based LC50s for mannitol, whose direct impacts should be strictly external and thus possibly related to osmotic effects, show no Ca dependence, unlike the increasing toxicity of Na salts at lower Ca. This indicates that the toxicity mechanisms for Na salts at low Ca are different and more potent than for mannitol. However, mannitol×NaCl mixtures show additive toxicity, indicating that NaCl also contributes to the mannitol mechanism. Further arguments for this mechanism being osmolarity-related include: 1) LC50s for these mixtures do not vary significantly on an osmolarity basis from each other or from mannitol-only and 2) for such diverse chemicals (Na, Cl, mannitol) to share a mechanism requires one such as osmolarity to which they all plausibly contribute.

252 At {Ca} ≈ 0.3 mM the LC50s for NaCl-only exposures have risen to converge with those
253 for mannitol, at which point they also become Ca independent, suggesting a "cap" on
254 osmolarity, until {Ca} is high enough to elicit Ca-driven toxicity. The osmolarity-based LC50s for
255 Na_2SO_4 reach the same osmolarity cap, but not until {Ca} ≈ 1 mM, due to the greater potency of
256 SO_4-related toxicity. Finally, these LC50s with putative osmolarity-related toxicity range from
257 250 to 350 mOsm/L, similar to blood osmolarities reported for freshwater teleost fish (270 to
258 350 mOsm/L; Hoar and Randall, 1969). If osmotic effects cause this toxicity, it is reasonable for
259 it to coincide with the transition from hypo-osmotic to hyper-osmotic. Therefore, the data
260 selected for osmolarity-related toxicity model development include mannitol-only exposures,
261 NaCl×mannitol mixtures, NaCl exposures at 0.3 mM ≤ {Ca} ≤ 10 mM, and Na_2SO_4 exposures at
262 1 mM ≤ {Ca} ≤ 10 mM.
263 Figure 2B provides the same data expressed as the sum of the total molar concentration
264 of each major ion plus the molar concentration of mannitol (not including other, negligible
265 components of the dilution water, which total ≪1 mM/L). This metric would equal osmolarity
266 if all components were completely dissociated and if solute behavior was ideal; this was
267 referred to as "nominal osmolarity" in Erickson et al. (2018). This terminology change was
268 made so that the nature of the metric is more clear. For the data used to develop the
269 osmolarity-related toxicity models in Figures 2A and 2B, total ion+mannitol concentration
270 ranges from virtually the same as osmolarity for mannitol-only exposures to about 20% higher
271 for Na_2SO_4-only exposures. This narrow (±10%) range makes this measure a good
272 approximation for osmolarity that is much easier to estimate.
273 ***Model formulation, parameterization, and performance***

Due to the absence of a Ca effect on the data with putative osmolarity-related toxicity (Figure 2), the proposed, activity-based model is simply a constant osmolarity. This value was set to the average of the selected LC50s in Figure 2A, which is 283 mOsm/L (n=20). All the data are within a factor of 1.27 of this value and the residual log standard deviation is 0.056, similar to the Ca/Mg model and to the inter-experimental log standard deviation of 0.047 for LC50s of tests with mannitol. The residual plot (Figure 2C) shows that the LC50s for mannitol, mannitol mixtures, and ion salts are consistent with this inter-experimental variability. There is a slight downward trend of residuals with Ca, but the slope for this trend by linear regression (Sigmaplot Version 14.0, Systat Software) is not statistically significant ($p>0.1$) and would cause a difference of only 15% over the entire data range.

Similarly, the proposed concentration-based model for osmolarity-related toxicity is the average total ion+mannitol concentration for the selected data in Figure 2B, which is 299 mM/L (n=20). For this model, all the data are within a factor of 1.22 of this average, the residual log standard deviation is 0.054, and the residual plot (Figure 2D) shows no trend. Therefore, unlike the Mg/Ca toxicity model, this concentration-based model for osmolarity-related toxicity performs as well as the activity-based model and is recommended for use given its much easier calculation.

Comparison to C. dubia

In contrast to the similar relationships formulated into the Mg/Ca models for both fathead minnows and *C. dubia* (Figure 1), the shape and scope of the osmolarity-related toxicity models proposed for fathead minnow differ greatly from the osmolarity-based models for *C. dubia* (Figure 2) due to a change in modeling approach. For fathead minnows, the osmolarity-related model focuses on toxicity that is plausibly due to osmotic effects. As such,

this model explains major ion toxicity over a limited Ca range, because more potent ion effects at lower Ca do not appear attributable to osmolarity per se even if they are well correlated.

For *C. dubia*, different Ca-dependencies for mannitol and NaCl are now known also to be true (Figure 2), but this was unknown when the *C. dubia* model was developed (Erickson et al. 2018). At that time, some *C. dubia* tests did suggest osmotic effects at some Ca (Mount et al., 2016; Erickson et al., 2017), but the use of osmolarity as the exposure metric at other Ca was based on good empirical correlation to the data and did not imply causation over the entire range. In addition, the model in Figure 2A for *C. dubia* also includes Ca-specific toxicity, which is repetitive of the Mg/Ca model and entails more complex calculations, which our present modeling efforts are trying to reduce.

In light of the evidence that osmolarity is not the cause of toxicity to *C. dubia* at lower Ca, further model development for *C. dubia* is warranted. Based on the evaluation of the Ca-dependence of mannitol toxicity to *C. dubia* in the current study (Supplemental Information in Erickson et al., 2022), Figure 2A provides a possible LC50 value (80 mOsm/L) for an osmolarity-related model for *C. dubia* analogous to that provided for fathead minnow. This is only meant to illustrate how *C. dubia* modeling could evolve to better align with the inferred mechanisms. Furthermore, this does not mean that the *C. dubia* models from Erickson et al. (2018) cannot be useful, but rather that they need to be viewed as more empirical and not fully reflecting current mechanistic understanding. Interestingly, this osmolarity-related toxicity value for *C. dubia* is similar to the internal osmolarity reported for *D. magna* (≈100 mOsm/L based on data reported by Morris et al., 2021), just as the osmolarity-related toxicity model for fathead minnow is similar to freshwater fish internal osmolarities (Hoar and Randall, 1969).

SULFATE-RELATED TOXICITY

Data for model development

The SO_4-related toxicity inferred in Erickson et al. (2022) involves exposures in which the anion is almost all SO_4 and Ca is below that at which toxicity is osmolarity related. Figure 3 therefore includes LC50 values from tests involving Na_2SO_4 or Na_2SO_4×$MgSO_4$ mixtures, with SO_4 and Ca plotted as activity in 3A and concentration in 3B. For both plots, the small symbols at higher Ca involve exposures for which the osmolarity-related toxicity model (Figure 2) would apply or that are transitional between osmolarity-related and SO_4-related toxicity. The remaining data with large symbols define a clear, strong Ca dependence for SO_4-related toxicity, with some apparent curvature for logSO_4 versus logCa. The slope differences between Figures 3A and 3B are expected as a result of activity coefficients decreasing and fraction complexation increasing as concentrations increase.

Model formulation, parameterization, and performance

To address curvature in the data, the models for SO_4-related toxicity use a hyperbolic formulation equivalent to that for Mg/Ca-related toxicity (Equation 1). The parameterized activity-based model for SO_4-related toxicity is:

$$LC50_{\{SO_4\}} = 10^{\left(2.16 - \frac{2.22}{\log\{Ca\}_M + 3.20}\right)} \quad \text{(Eq. 6)}$$

The log residual standard deviation for this model is 0.065, moderately higher than for the models for Mg/Ca-related and for osmolarity toxicities. This does not indicate model error, but rather a larger inter-experimental variability for SO_4-related toxicity, which has a log standard deviation for $\{SO_4\}$-based LC50s for repeated Na_2SO_4 tests in ALSW of 0.070 (n=6). This variability is evident in Figure 2A, where LC50s in ALSW for Na_2SO_4 range from similar to those

for NaCl to a factor of 2 lower. The residual plot in Figure 3C shows no systematic trends with Ca and no indication of more variability than expected from the inter-experimental log standard deviation.

The parameterized concentration-based model for SO_4-related toxicity is:

$$LC50_{[SO_4]} = 10^{\left(3.80 - \frac{7.70}{\log[Ca]_M + 3.92}\right)} \quad \text{(Eq. 7)}$$

The log residual standard deviation for this model is 0.082, higher than for the activity-based model. This is due to a large inter-experimental log standard deviation for $[SO_4]$-based LC50s (0.100; n=6), which is greater than for $\{SO_4\}$-based LC50s because increased complexation and decreased activity coefficients at higher concentrations cause $\{SO_4\}$ to vary less than $[SO_4]$. However, the uncertainty associated with this is still relatively modest, two residual standard deviations corresponding to factor of 1.45 compared to 1.35 for the activity-based model. The residual plot in Figure 3D also affirms that deviations from the model are consistent with the inter-experimental variability and are independent of Ca.

Comparison to C. dubia

For *C. dubia*, this SO_4-related toxicity was not observed; rather, toxicities of NaCl and Na_2SO_4 were not significantly different on an osmolarity basis (Mount et al. 2016; Erickson et al. 2018). Like the toxicity associated with high pH/alkalinity, this difference between the species might mean that fathead minnows are subject to a mechanism of toxicity to which *C. dubia* are less susceptible, but it might simply mean the greater sensitivity of *C. dubia* causes it to succumb to other ion effects before lethal levels of SO_4 are reached.

MULTI-ION TOXICITY AT LOW CALCIUM

Data for model development

The larger symbols in Figure 4 include fathead minnow LC50s for NaCl and Na×Na salt mixtures at lower Ca. As discussed in Erickson et al. (2022) and as illustrated in Figure 2, these data appear to reflect a mechanism separate from osmolarity-related toxicity, sulfate-related toxicity, and high pH/alkalinity effects of $NaHCO_3$-dominated exposures. Data with smaller symbols are provided to show the transition to osmolarity-related toxicity, and were not used for modeling this low Ca mechanism. The LC50 for Na gluconate is included to show the agreement with the inorganic salts, but also was not used for model development.

The larger symbols in Figure 4 also include Na×Mg salt mixtures in which the fraction Mg is low enough that Mg-specific toxicity is not expected based on the Mg/Ca model. These data need to be considered in the modeling due to the partial additivity in these mixtures (Erickson et al., 2022); i.e., Mg salts contribute to the toxicity of Na salts when there is insufficient Mg to produce Mg-specific toxicity. Data for NaCl×KCl mixtures with lower proportions of K are similarly included.

For the other mechanisms being modeled (Figure 1-3), toxicity can be attributed to specific causes, which then dictate the appropriate exposure metrics for model development (specific ions or osmolarity). In contrast, the explicit cause of toxicity for the ion combinations in Figure 4 is not clear, so multiple possible metrics were considered. Figure 4 presents the data on the basis of three candidate metrics. Because Na is the dominant cation for this set of data, Figure 4A is on the basis of {Na} vs {Ca} to consider how well this describes the toxicity despite it not considering contributions of other ions. To address whether including multiple ions improves description of the data, metrics involving all major ions are also presented.

Because of the importance of activity for describing other toxicity mechanisms, one metric is the sum of the activities of the uncomplexed ions (Figure 4B). And to provide a concentration-basis for the model, another metric is the sum of the total concentrations of the ions (Figure 4C). Such metrics are not mechanistically based because they do not identify causative ions and make the assumption that the relative potencies of the ions are the same. Therefore, this modeling is strictly empirical and the utility of these metrics must be judged based only on overall fit relative to data uncertainty.

Model formulation, parameterization, and performance

For the exposure metric of {Na}, the data in Figure 4A show a strong correlation to Ca with some possible curvature. To address this curvature, the same hyperbolic formulation as for Mg/Ca-related toxicity (Equation 1) was used. The parameterized model is:

$$LC50_{\{Na\}} = 10^{\left(3.18 - \frac{4.38}{\log\{Ca\}+4.39}\right)} \quad \text{(Eq. 8)}$$

Using {Na} as the metric does not address involvement of multiple ions and results in substantial residual errors (Figure 4D). A notable set of negative residuals (circled in Figure 4D) are for equipotent mixtures of Na salts with Mg and K salts, for which Mg and K activities are too low for Mg-specific or K-specific toxicity, but high enough to contribute to the mixture toxicity. Residuals for several other treatments are also substantial. This results in a log residual standard deviation, 0.081, that is much higher than for the Mg/Ca and osmolarity models and is even higher than for the activity-based SO_4 model. The indicator of inter-experimental variability most relevant to the present model is for {Na}-based LC50s for NaCl in ALSW, for which the repeated tests have a log standard deviation of only 0.032. Although this

406 probably underestimates variability for all the exposure conditions in this data set, it
407 nonetheless demonstrates problems with the model.
408 Addressing the issue of multiple ions using the sum of the activities of the uncomplexed
409 anions (Figure 4B) produces the following model equation:

410 $$LC50_{ActivitySum} = 10^{\left(3.69 - \frac{5.48}{\log\{Ca\}+4.67}\right)}$$ (Eq. 9)

411 Because other ions are now included in the exposure metric, the residual plot (Figure 4E) does
412 show some improvement for the equipotent mixtures of Na salts with Mg and K salts, but the
413 overall log residual standard deviation for the model (0.072) remains considerably higher than
414 the inter-experimental log standard deviation (0.042) estimated from repeated tests in ALSW
415 for various salts in this data set. Using activity sums for smaller subsets of the major ions (e.g.,
416 cations only) does not improve performance (data and analyses not shown). Model
417 performance could be improved by using a weighted sum of the activities, but this risks
418 overfitting of the data and not providing meaningful mechanistic inferences, and also involves
419 greater computational complexity.
420 Using total ion concentration as the exposure metric yields a parameterized model of:

421 $$LC50_{TotalIonConc} = 10^{\left(2.64 - \frac{0.391}{\log[Ca]+1.80}\right)}$$ (Eq. 10)

422 This provides improved adherence to the data (Figure 4C) and reduced residuals (Figure 4F),
423 although the extremely tight correlation at [Ca] < 0.1 mM is likely happenstance to some
424 extent, given the low residuals relative to inter-experimental variability (Figure 4E). The log
425 residual standard deviation for this model is 0.052, consistent with the inter-experimental log
426 standard deviation of 0.055 for total ion-based LC50s for repeated tests of various salts in

ALSW. Although this model has less mechanistic rationale than the other models, it does provide a good empirical fit to these data. In addition, because it uses total ion concentration, the osmolarity-related toxicity model in Figure 2B can be compared in Figure 4C, showing the intersection of the mechanisms.

Comparison to C. dubia

For *C. dubia*, toxicity of Na salts and various salt mixtures, except those dominated by Mg or K, were described by "general ion toxicity" models using osmolarity or nominal osmolarity (Erickson et al., 2018). These models cover the entire range of Ca and do not explicitly address mechanistic differences at lower Ca as done here for fathead minnow, instead using osmolarity as a correlate across all Ca. However, at low Ca, they are similar to the fathead minnow models in Figure 4 in that they involve a strongly Ca-dependent toxicity of Na salts and mixtures that is related to multiple ions. The comparison of the models in Figure 4C shows similar trends of toxicity for the two species at lower Ca, with *C. dubia* being about 2.5 to 3 times more sensitive.

MODEL APPLICATION AND DEVELOPMENT ISSUES

The relationships for acute toxicity of major ions to fathead minnow described in the present paper and the companion paper (Erickson et al. 2022) provide a good framework for understanding major ion toxicity in this species, but application of this to risk assessments requires consideration of various additional issues.

High pH/alkalinity and potassium-related toxicities

As noted in the Introduction, two of the apparent mechanisms inferred by Erickson et al. (2022), high pH/alkalinity effects and K-specific toxicity, were not subject to model development due to insufficiently-resolved dependencies on certain exposure variables.

450 However, these mechanisms are relevant to whether the models for other mechanisms should
451 be applied to a particular exposure. This need can be partly satisfied by using screening values
452 for determining whether high pH/alkalinity effects or K-specific toxicity might be of concern.
453 For K-specific toxicity, Erickson et al. (2022) found a minimum activity-based LC50 of
454 7.8 mM K, for the low-ion test water (⅓ strength ALSW) having the highest K potency. For
455 exposures with less than this concentration, the models for other mechanisms can be applied
456 without concerns about possible K toxicity.
457 The enhanced toxicities in $NaHCO_3$ and $MgCO_3$ tests relative to their respective Cl salts
458 involved both pH > 9.1 and $\{HCO_3\}$ > 15 mM (Erickson et al., 2022). If either of these screening
459 criteria are not met, these effects should not be of concern, because 1) lowering pH allowed
460 tolerance to $\{HCO_3\}$ as high as 30 mM and 2) reducing $\{HCO_3\}$ to <13 mM in mixtures allowed
461 tolerance to pH as high as 9.2 (Erickson et al., 2022).
462 ***Model application procedures***
463 The mixture experiments presented by Erickson et al. (2022) suggest that each of the
464 mechanisms modeled in this paper are independent of the others. Thus, to estimate the
465 toxicity in an exposure water of interest, a relative toxicity predicted by each model is
466 separately calculated by dividing the value of model's exposure metric in the water of interest
467 by the predicted LC50 from the model (i.e., toxic units or TU). For example, for the activity-
468 based SO_4 model, $\{SO_4\}$ would be estimated for the exposure water and divided by the
469 predicted $LC50_{\{SO4\}}$ from Equation 6 for the {Ca} of the water. Due to the independence of the
470 mechanisms, whatever mechanism has the highest TU would provide the estimated toxicity for
471 the water. A comparable TU calculation could be made for the screening values for K-specific
472 toxicity and high pH/alkalinity effects to determine if these mechanisms might affect the

473 applicability of the models for the other mechanisms. This is comparable to considering any set
474 of toxicants in an exposure water and calculating TUs to identify the ones of concern.
475 Table 1 provides an example of such model application for a set of acute LC50s for major
476 ion salts and mixtures to fathead minnows from Mount et al. (1997), which also provides a test
477 of model predictability for a data set independent of the present study. Table 1 lists average
478 LC50s, as mg/L, from Mount et al. (1997) for 16 single salts and equimolar binary mixtures.
479 These LC50s and the ion content of the dilution water were converted to molarity for each ion,
480 total ion concentrations/nominal osmolarities were calculated, and ion activities were
481 estimated as described in Erickson et al. (2022). The predicted LC50 for each model was
482 calculated (Equations 3, 6, 7, and 10, and the screening values for K-related toxicity and high
483 pH/alkalinity effects) and divided into its exposure metric in the test water to provide a
484 predicted TU for each water and mechanism.
485 The predicted TUs for each mechanism and test water are listed in Table 1, with the
486 highest TU for each test water highlighted and compiled in the last column. With the exception
487 of the NaCl×$MgCl_2$ mixture, this procedure assigns each salt and mixture to an appropriate
488 model, with TUs varying from 0.61 to 1.54, reasonable deviations from 1.0 for inter-study
489 variability, especially considering the range of starting ages used by Mount et al. (1997) relative
490 to that of Erickson et al. (2022). For the NaCl×$MgCl_2$ mixtures, both the Mg-driven and the
491 multi-ion mixture models show a TU of about 0.5. Although these TUs are still substantial, this
492 underprediction might reflect the uncertainty of the interactions in these mixtures (Erickson et
493 al. 2022).
494 In addition to assessing TUs in exposure waters of interest, the models presented here
495 can also be used in prospective assessments to predict toxic values for the various exposure

metrics as a function of Ca. For such an application, if two different metrics are both at toxic levels, hazard might be underestimated for independent mechanisms, due to each contributing some toxicity that in combination causes greater toxicity than either alone. In such a case, interactions between independent mechanisms can be addressed as described in Erickson et al. (2018) and references therein. However, due to the steep exposure-response relationships observed for major ions, it should be rare for two mechanisms to have sufficiently similar effects to cause substantial underprediction of toxicity.

Scope of applicability – range of exposure conditions for major ion assessments

In order to elucidate various ion toxicity interactions and mechanisms, the experiments in Erickson (2022) involved a wide range of major ion mixture compositions, some with unusual ion ratios unlikely to be of concern in actual assessments, and the models reflect this wide range. Although this broad scope does not preclude model application, simpler models could be developed that focus on ranges of ionic mixtures more likely to occur. For example, Erickson et al. (2018) validated the *C. dubia* models using additional toxicity tests on complex mixtures mimicking reported major ion elevations in various aquatic systems. Although this was a limited set of exposures, substantial Mg exposures did not occur without at least some elevation of Ca, suggesting that the lower end of the Mg/Ca model might not be needed. Even for NaCl-dominated road salt runoff into receiving waters with low Ca, how much concomitant Ca elevation might occur from other substances on the road? Similarly, will high SO_4 exposures occur in the absence of elevated Ca (e.g., Ca from neutralization of acid mine drainage), so that the low Ca, SO_4-related toxicity model would have limited utility? And are the high pH/alkalinity effects on fathead minnows in the present study of any practical concern? Although beyond the scope of the present study, a comprehensive review that establishes the

519 range of likely exposures that should be addressed by major ion toxicity assessment methods
520 could focus further model development.

521 ***Scope of applicability – other datasets, species, and endpoints***

522 As currently formulated, the models in Figures 1-4 reflect toxicity data only from
523 Erickson et al. (2022). To provide a more robust and representative model, consideration
524 should be given to further developing the models using additional major ion toxicity data for
525 fathead minnows (e.g., Mount et al., 1997).

526 Beyond application to acute toxicity to fathead minnow, the models in Figures 1-4 could
527 be useful in assessing risks for other species and endpoints. Fathead minnows are very similar
528 to *C. dubia* regarding the shape of the toxicity relationships for the Mg/Ca model (Figure 1),
529 which could extend to other species and endpoints. The current perspective on osmolarity-
530 related toxicity and mixture toxicity at low Ca (Figures 2 and 4) could be used to improve
531 models for *C. dubia*, and interpreting responses for other species and endpoints. However,
532 fathead minnow and *C. dubia* differ in other respects, including the SO_4-related and K-related
533 toxicities and the effects of high pH/alkalinity, which leaves uncertain how these factors may
534 apply to other species and endpoints. Therefore, these fathead minnow models can provide
535 broader insights for major ion risk assessments, but such application requires care.

536 ***Other exposure metrics for further model development***

537 Although the model in Equation 10 and Figure 4C provides a good empirical description
538 for a toxicity mechanism distinct from the other mechanisms, the exposure metric of total ion
539 concentration is not mechanistically satisfying in that it doesn't identify specific causative
540 agents and doesn't address possible potency differences among ions. This model would be
541 strengthened by a better understanding of this multiple-ion mechanism – which ions are

actually contributing to this toxicity and how? One possibility is that all ions can affect the electrical potential across cellular membranes, which is important to ion transport and cell function. Recent efforts (EPRI, 2018; Wood et al., 2020; Po and Wood, 2021) have examined the impact of major ions on transepithelial potential and its possible relationship to major ion toxicity. Because all ions influence transepithelial potential, it is a potentially attractive explanation for the multi-ion toxicity at low Ca (Figure 4), and might have implications for other mechanisms as well. However, it is unlikely that this single mechanism could explain the range of toxicity relationships and interactions observed by Erickson et al. (2022), in particular the independence of effects for certain salt pairs.

Another exposure metric that warrants discussion is conductivity. Conductivity has an obvious general connection to the ion content of exposure waters and is an attractive monitoring tool in being inexpensive and easy to measure. This measure has been used in interpreting field data on impacts of elevated ions on aquatic communities and has attracted interest as a basis for regulations (Pond. et al., 2008; Cormier and Suter, 2013; Cormier et al., 2013, 2018). Such field-based methods also have the benefit of addressing a broader diversity of organisms than can be tested in the laboratory.

However, the specific conductivities of individual ions vary widely and have uncertain connections to their toxicological potencies; as a result, major ion toxicities expressed as conductivity can vary with the mixture composition even more than the metrics used in the present paper. Mount et al. (2016) showed that conductivity-based LC50s for *C. dubia* varied widely among different major ion salts and dilution waters and that conductivity was much less explanatory of toxicity than {Mg} for Mg salts and osmolarity for Na salts. The same is true for fathead minnows in this study. For example, Erickson et al. (2022) reported that the average

{Mg}-based LC50 in ALSW for $MgSO_4$ was 10% lower than that for $MgCl_2$, in accordance with the Ca effect on Mg toxicity. In contrast, conductivity-based LC50s computed here from the raw data of Erickson et al. (2022) averaged 30% higher for $MgSO_4$. Therefore, the formulation and scope of applicability of field-based conductivity limits should be informed by the relationships demonstrated in toxicological studies, or restricted to relative ion composition close to the data from which they were developed. Conversely, field-based impacts on aquatic communities can inform the applicability to risk assessments of laboratory-based tools such as the models of the present study.

REFERENCES

Berger E, Frör O, Schäfer RB. 2019. Salinity impacts on river ecosystem processes: a critical mini-review. *Phil Trans R Soc B* 374:20180010. http://dx.doi.org/10.1098/rstb.2018.0010

Cañedo-Argüelles M. 2020. A review of recent advances and future challenges in freshwater salinization. *Limnetica* 39(1):185-211. http://dx.doi.org/10.23818/limn.39.13

Cañedo-Argüelles M, Kefford B, Schäfer R. 2019. Salt in freshwaters: causes, effects and prospects - introduction to the theme issue. *Phil Trans R Soc B* 374:20180002. http://dx.doi.org/10.1098/rstb.2018.0002

Cormier SM, Suter, GW II. 2013. A method for deriving water-quality benchmarks using field data. *Environ Toxicol Chem* 32:255-262. https://doi.org/10.1002/etc.2057

Cormier SM, Suter, GW II, Zheng L. 2013. Derivation of a benchmark for freshwater ionic strength. *Environ Toxicol Chem* 32:263-271. https://doi.org/10.1002/etc.2064

Cormier SM, Zheng L, Flaherty CM. 2018. A field-based model of the relationship between extirpation of salt-intolerant benthic invertebrates and background conductivity. *Sci Total Environ* 633:1629-1636. https://doi.org/10.1016/j.scitotenv.2018.02.044

Electric Power Research Institute. 2018. Multi-Ion Toxicity Review: Data Analyses and Ongoing Model Framework Development. Report #3002013924, EPRI, Palo Alto, Ca.

Erickson RJ, Mount DR, Highland TL, Hockett JR, Hoff DJ, Jenson CT, Norberg-King TJ, Peterson KN. 2017. The acute toxicity of major ion salts to *Ceriodaphnia dubia*. II. Empirical relationships in binary salt mixture toxicity tests. *Environ Toxicol Chem* 36:1525-1537. http://dx.doi.org/10.1002/etc.3669

595 Erickson RJ, Mount DR, Highland TL, Hockett JR, Hoff DJ, Jenson CT, Norberg-King TJ, Peterson
596 KN. 2018. The acute toxicity of major ion salts to *Ceriodaphnia dubia*. III. Modeling the toxicity
597 of major ion mixtures. *Environ Toxicol Chem* 37:247-259. http://dx.doi.org/10.1002/etc.3953

598 Erickson RJ, Mount DR, Highland TL, Hockett JR, Hoff DJ, Jenson CT, Norberg-King TJ, Forsman
599 BB. 2022. Acute Toxicity of Major Geochemical Ions to Fathead Minnows (Pimephales
600 promelas). Part A. Observed Relationships for Individual Salts and Salt Mixtures. *Environ*
601 *Toxicol Chem* VV:ppp-ppp.

602 Hintz DH; Relyea RA. 2019. A review of the species, community, and ecosystem impacts of
603 road salt salinisation in fresh waters. *Freshw Biol* 64:1081–1097.
604 http://dx.doi.org/10.1111/fwb.13286

605 Hoar WS, Randall DJ. 1969. *Fish Physiology Vol I. Excretion, Ionic Regulation, and Metabolism*.
606 Academic Press, New York.

607 Kaushal SS, Likens GE, Pace ML, Reimer JE, 30 others. 2021. Freshwater salinization syndrome:
608 from emerging global problem to managing risks. *Biogeochemistry* 154:255-292.
609 https://doi.org/10.1007/s10533-021-00784-w

610 Morris C, Sakarya M, Koh O, O'Donnell M. 2021. Alterations in hemolymph ion concentrations
611 and pH in adult Daphnia magna in response to elevations in major ion concentrations in
612 freshwater. *Environ Toxicol Chem* 40:366-379. http://dx.doi.org/10.1002/etc.4919

613 Mount DR, Gulley DD, Hockett JR, Garrison TD, Evans JM. 1997. Statistical models to predict
614 the toxicity of major ions to *Ceriodaphnia dubia*, *Daphnia magna* and *Pimephales promelas*

(fathead minnow). *Environ Toxicol Chem* 16:2009-2019.
http://dx.doi.org/10.1002/etc.5620161005

Mount DR, Erickson RJ, Highland TL, Hockett JR, Hoff DJ, Jenson CT, Norberg-King TJ, Peterson KN, Wisniewski S. 2016. The acute toxicity of major ion salts to *Ceriodaphnia dubia*. I. The influence of background water chemistry. *Environ Toxicol Chem* 35:3039-3057.
http://dx.doi.org/10.1002/etc.3487

Po BHK, Wood CM. 2021. Trans-epithelial potential (TEP) response as an indicator of major ion toxicity in rainbow trout and goldfish exposed to 10 different salts in ion-poor water. Environ. Pollut. 276. https://doi.org/10.1016/j.envpol.2021.116699

Pond GJ, Passmore ME, Borsuk FA, Reynolds L, Rose CJ. 2008. Downstream effects of mountaintop coal mining: Comparing biological conditions using family- and genus-level macroinvertebrate bioassessment tools. *J N Am Benthol Soc* 27:717-737.
https://doi.org/10.1899/08-015.1

Schuler MS, Cañedo-Argüelles M, Hintz WD, Dyack B, Birk S, Relyea RA. 2019. Regulations are needed to protect freshwater ecosystems from salinization. *Phil Trans R Soc B* 374:20180019.
http://dx.doi.org/10.1098/rstb.2018.0019

Wood CM, McDonald MD, Grosell M, Mount DR, Adams WJ, Po BHK, Brix KV. 2020. The potential for salt toxicity: Can the trans-epithelial potential (TEP) across the gills serve as a metric for major ion toxicity in fish? Aquat.Toxicol. 226:105568.
https://doi.org/10.1016/j.aquatox.2020.105568.

636 **Table 1.** Application of models and screening values from the present study for various mechanisms of
637 major ion acute toxicity to fathead minnows. Reported LC50s (mg/L basis) from Mount et al. (1997)
638 were used to compute toxic units relative to predictions. Highlighted toxic units identify the mechanism
639 with the greatest sensitivity that defines the overall toxic unit for each exposure.

Major Ion Salt or Mixture	LC50 (mg/L)	Toxic Units for Toxicity Mechanism						
		Ca/Mg	Osmolarity	SO_4 Low Ca	Multi-Ion Low Ca	K	High pH/Alk	Overall
NaCl	6390	0.020	0.745	0.017	0.998	0.005	0.064	0.998
Na_2SO_4	7960	0.013	0.576	1.536	0.771	0.005	0.062	1.536
$NaHCO_3$	850	0.028	0.081	0.029	0.109	0.006	0.641	0.641
KCl	880	0.033	0.093	0.025	0.124	1.296	0.076	1.296
K_2SO_4	680	0.028	0.053	0.157	0.071	0.852	0.076	0.852
$MgCl_2$	2120	0.713	0.237	0.013	0.317	0.005	0.060	0.713
$MgSO_4$	2820	0.609	0.170	0.504	0.228	0.005	0.062	0.609
$CaCl_2$	4630	0.974	0.432	0.003	0.385	0.005	0.050	0.974
$NaClxNa_2SO_4$	6090	0.016	0.577	0.532	0.773	0.005	0.064	0.773
$NaClxNaHCO_3$	2540	0.025	0.260	0.023	0.348	0.006	0.952	0.952
$Na_2SO_4xNaHCO_3$	4060	0.017	0.319	0.438	0.427	0.005	1.416	1.416
$MgCl_2xMgSO_4$	2800	0.741	0.239	0.212	0.320	0.005	0.060	0.741
$NaClxCaCl_2$	6460	0.613	0.675	0.004	0.609	0.005	0.053	0.675
$NaClxMgCl_2$	3160	0.513	0.361	0.014	0.483	0.005	0.061	0.513
$CaCl_2xMgCl_2$	5250	1.269	0.528	0.003	0.480	0.005	0.050	1.269
$Na_2SO_4xMgSO_4$	4800	0.451	0.317	0.864	0.424	0.005	0.062	0.864

640

641

642 **FIGURE CAPTIONS**

643 **Figure 1.** Data and models for Ca/Mg-related acute toxicity to fathead minnows. Figure
644 includes all LC50s for individual Mg and Ca salts, Mg×Mg salt mixtures, and Mg×Ca salt mixtures
645 from Erickson et al. (2022), plotted as Mg activity versus Ca activity in Panel A and as Mg
646 concentration versus Ca concentration in Panel B. The solid lines denote the fit of the LC50s
647 with larger symbols to a model assuming additivity of Mg and Ca, superimposed on a hyperbolic
648 function (dashed lines) for the dependence of the Mg toxicity on Ca in the absence of Ca toxicity
649 (Equations 4-5). Smaller symbols denote LC50s not used in model development, including Mg
650 gluconate, Ca gluconate, and exposures dominated by $MgCO_3$. The dotted lines provide
651 analogous models for *C. dubia* (Erickson et al. 2018). Panels C and D provide the residual log
652 deviations of the LC50s from the model lines in Panels A and B, respectively; shaded areas
653 represent ± 2 inter-experimental log standard deviations for repeated tests in the same dilution
654 water. Upward and downward arrows respectively denote LC50s slightly greater or lower than
655 plotted points. In figure legend, symbols for mixture experiments are for the single chemical
656 tests and the arrows represent the mixture tests with colors graded as appropriate.

657 **Figure 2.** Data and models for osmolarity-related acute toxicity to fathead minnows. Plot
658 includes all LC50s for individual Na and Ca salts, Na×Na salt mixtures, Na×Ca salt mixtures,
659 mannitol, and Na×mannitol mixtures from Erickson et al. (2022), plotted as osmolarity versus Ca
660 activity in Panel A and total ion + mannitol concentration versus Ca concentration in Panel B.
661 LC50s used for the osmolarity-related models are the larger symbols for mannitol, Na×mannitol
662 mixtures, and Na salt toxicity for certain ranges of Ca (see text). Solid lines denote average
663 values for these larger symbols (Ca-independent model). Smaller symbols denote LC50s not
664 used in model development that are associated with other mechanisms of toxicity. The dotted
665 lines show models from Erickson et al. (2018) for *C. dubia* that use osmolarity as the exposure
666 metric, but are not restricted to osmolarity-related toxicity. The dashed line in Panel A denotes
667 an alternative, Ca independent osmolarity-related model for *C. dubia*, based on mannitol data
668 (black stars). Panels C and D provide the residual log deviations of the LC50s from the model

669 lines in Panels A and B, respectively; shaded areas represent ±2 inter-experimental log standard
670 deviations for repeated tests in the same dilution water. Upward arrow denotes LC50s slightly
671 greater than plotted point. In figure legend, symbols for mixture experiments are for the single
672 chemical tests and the arrows represent the mixture tests with colors graded as appropriate.
673 **Figure 3.** Data and models for sulfate-related acute toxicity to fathead minnows. Plot includes
674 all LC50s for Na_2SO_4 and Na_2SO_4×MgSO4 mixtures from Erickson et al. (2022), plotted as SO_4
675 activity versus Ca activity in Panel A and SO_4 concentration versus Ca concentration in Panel B.
676 Smaller symbols denote tests at higher Ca that are associated with the osmolarity-related
677 toxicity in Figure 2 and not used for SO_4-related toxicity model development. Solid lines denote
678 the fit of the LC50s with larger symbols to a model assuming a hyperbolic relationship of SO_4 to
679 Ca (Equations 6-7). Panels C and D provide the residual log deviations of the LC50s from the
680 model lines in Panels A and B, respectively; shaded areas are ±2 interexperimental standard
681 deviations for repeated tests in the same dilution water.
682 **Figure 4.** Data and models for multi-ion acute toxicity to fathead minnows at low Ca. Plot
683 includes all LC50s for single-salt tests with NaCl and Na gluconate and all mixture tests with
684 Na×Na salts, Na×Mg salts, Na×K salts from Erickson et al. (2022), excluding mixtures dominated
685 by HCO_3, SO_4, Mg, and K and thus subject to other mechanisms. LC50s are plotted as Na activity
686 versus Ca activity in Panel A, a sum of major ion activities versus Ca activity in Panel B, and the
687 sum of total ion concentrations versus Ca concentration in Panel C. Smaller symbols for NaCl at
688 higher Ca denote LC50s not used in model parameterization that are associated with the
689 osmolarity-related toxicity in Figure 2. Solid lines denote fit of the LC50s to a model assuming a
690 hyperbolic relationship of the various exposure metrics to Ca (Equations 8-10). The dashed line
691 is the total ion-based model for osmolarity-related toxicity from Figure 2B. The dotted line in
692 Panel C is a portion of the total ion-based model from Erickson et al. (2018) for *Ceriodaphnia.*
693 *dubia*. Panels D, E, and F provide the residual deviations of the data from the model lines in
694 Panels A, B, and C, respectively; shaded areas are ±2 inter-experimental standard deviations for
695 repeated tests in the same dilution water. The circled data in Panel D highlight large negative

residuals for equitoxic mixtures of Na salts with Mg and K salts. In figure legend, symbols for mixture experiments are for the single chemical tests and the arrows represent the mixture tests with colors graded as appropriate.

Figure 1.

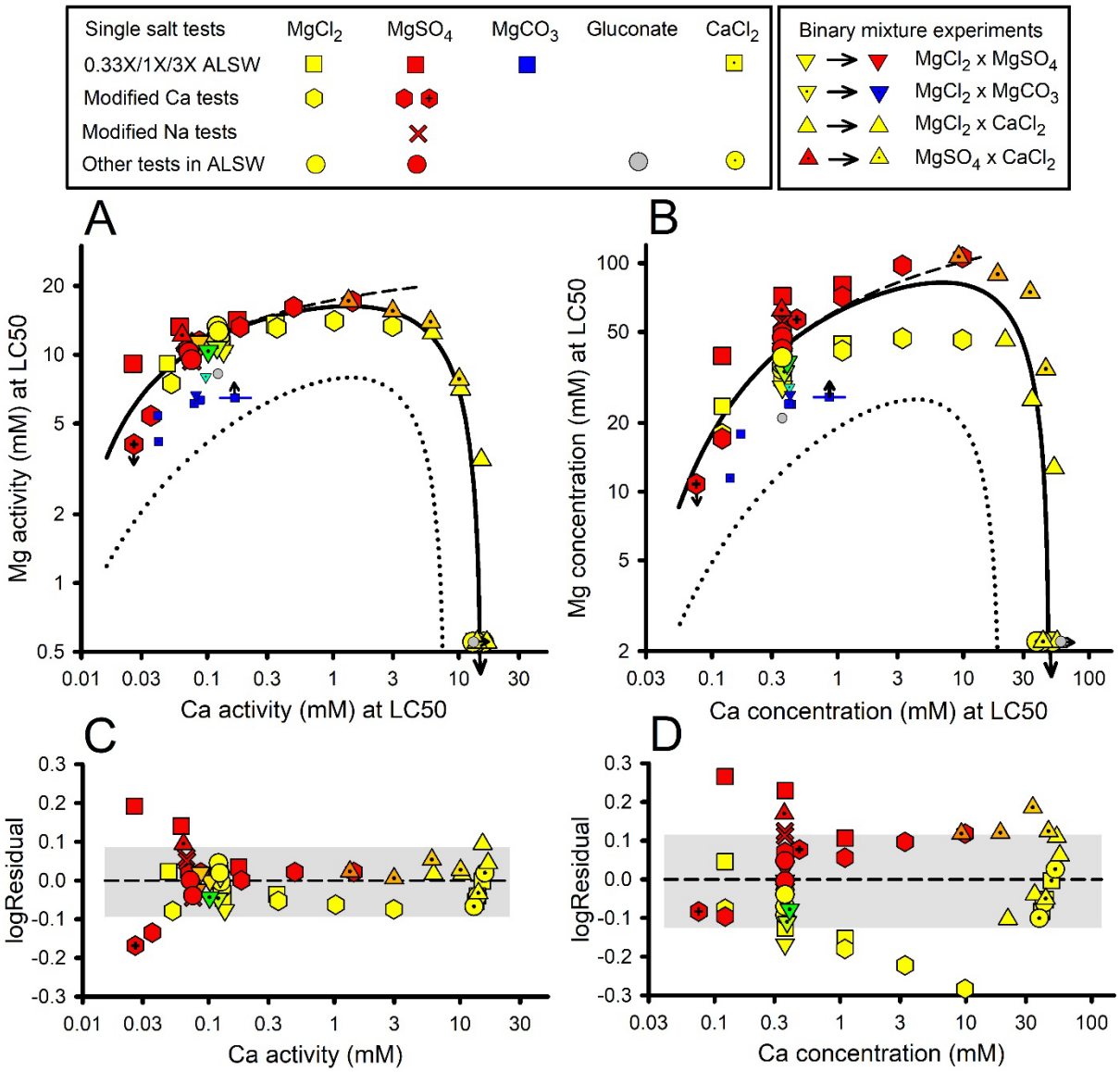
Single salt tests
MgCl2
MgSO4
MgCO3
Gluconate
CaCl2
0.33X/1X/3X ALSW
Modified Ca tests
Modified Na tests
Other tests in ALSW
Binary mixture experiments
MgCl2 x MgSO4
MgCl2 x MgCO3
MgCl2 x CaCl2
MgSO4 x CaCl2
A
Mg activity (mM) at LC50
Ca activity (mM) at LC50
B
Mg concentration (mM) at LC50
Ca concentration (mM) at LC50
C
logResidual
Ca activity (mM)
D
logResidual
Ca concentration (mM)

Figure 2

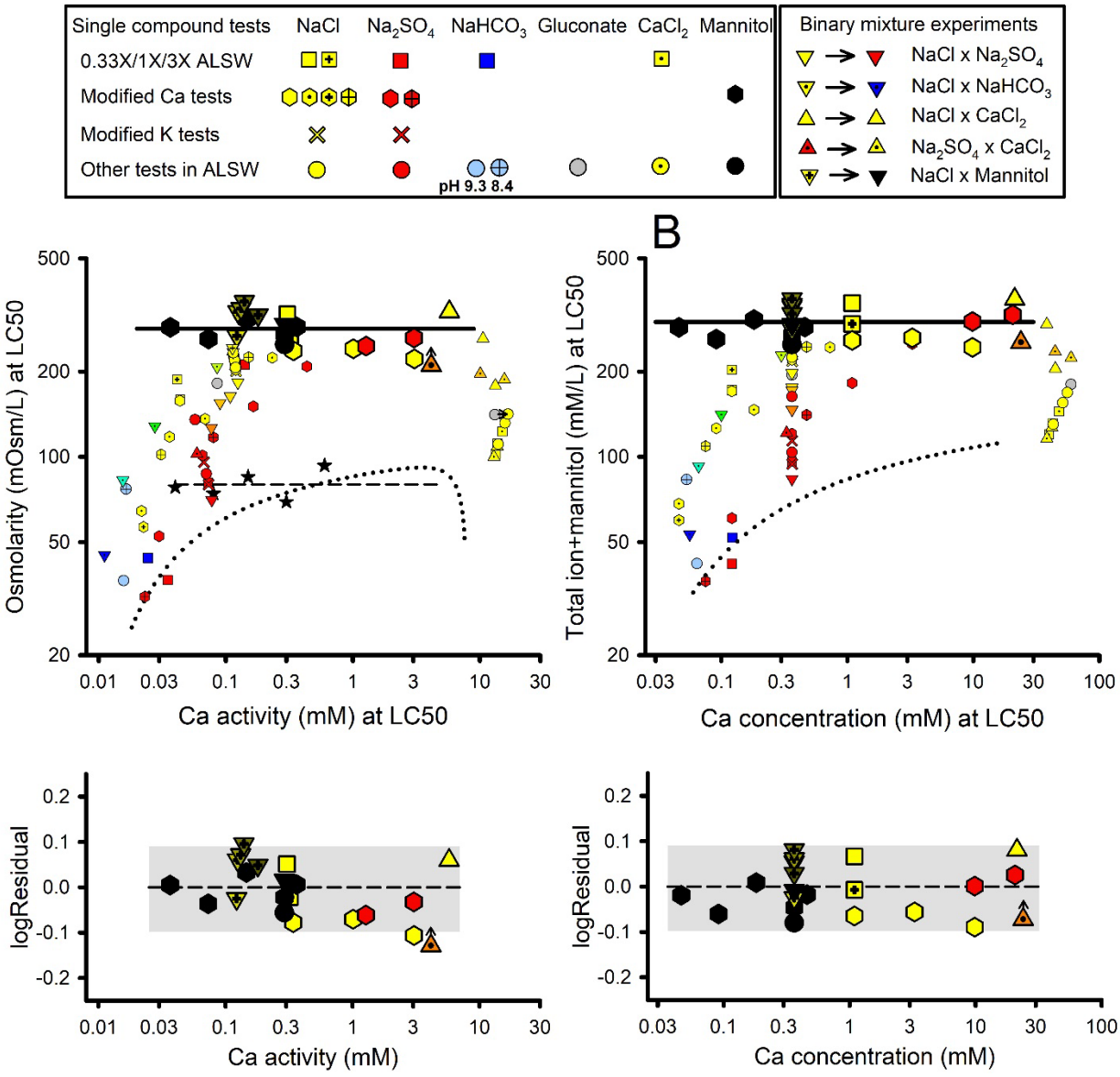

703

704

Figure 3

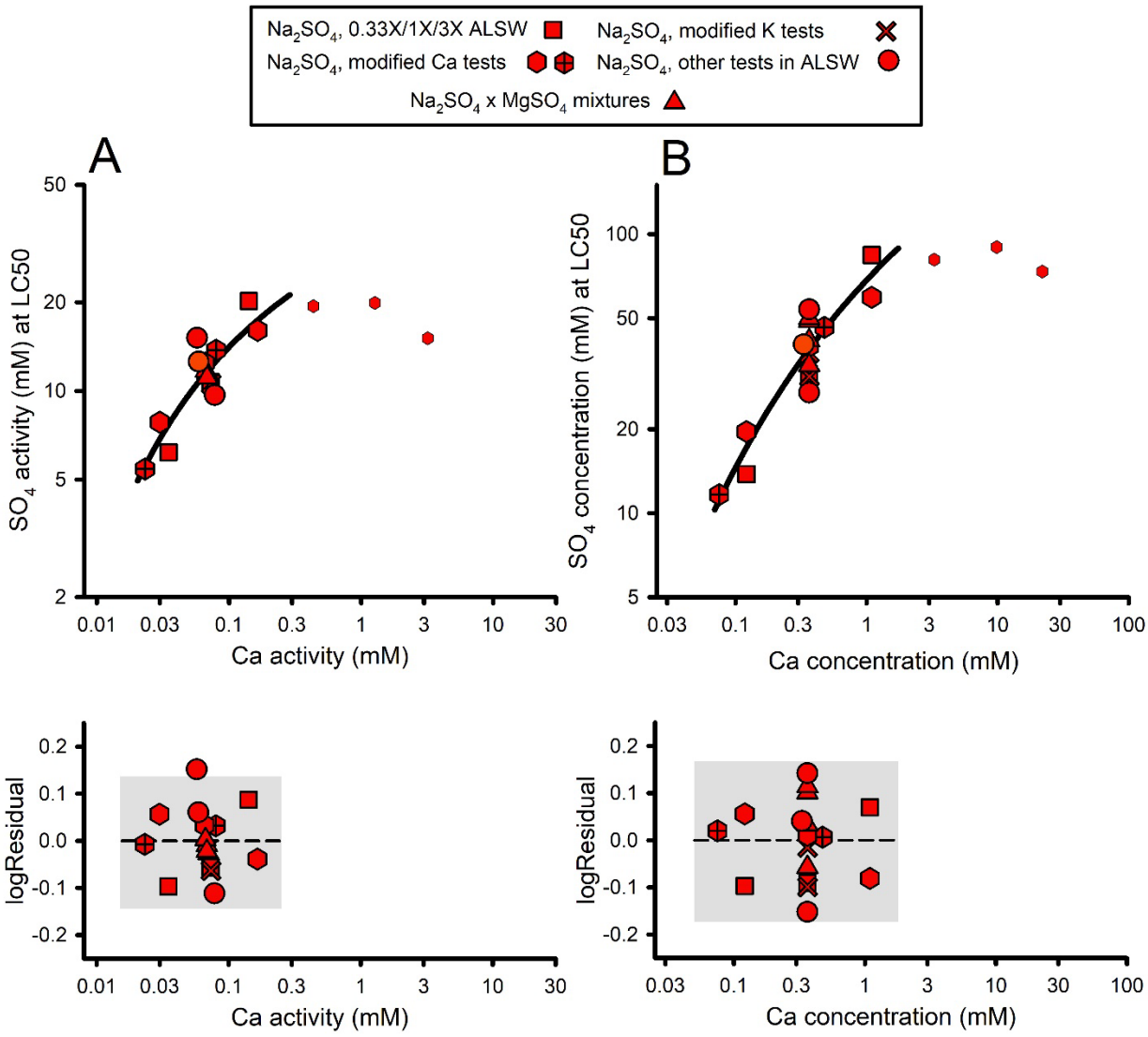
Na2SO4, 0.33X/1X/3X ALSW
Na2SO4, modified K tests
Na2SO4, modified Ca tests
Na2SO4, other tests in ALSW
Na2SO4 x MgSO4 mixtures
A
B
SO4 activity (mM) at LC50
SO4 concentration (mM) at LC50
Ca activity (mM)
Ca concentration (mM)
logResidual
Ca activity (mM)
Ca concentration (mM)

Figure 4

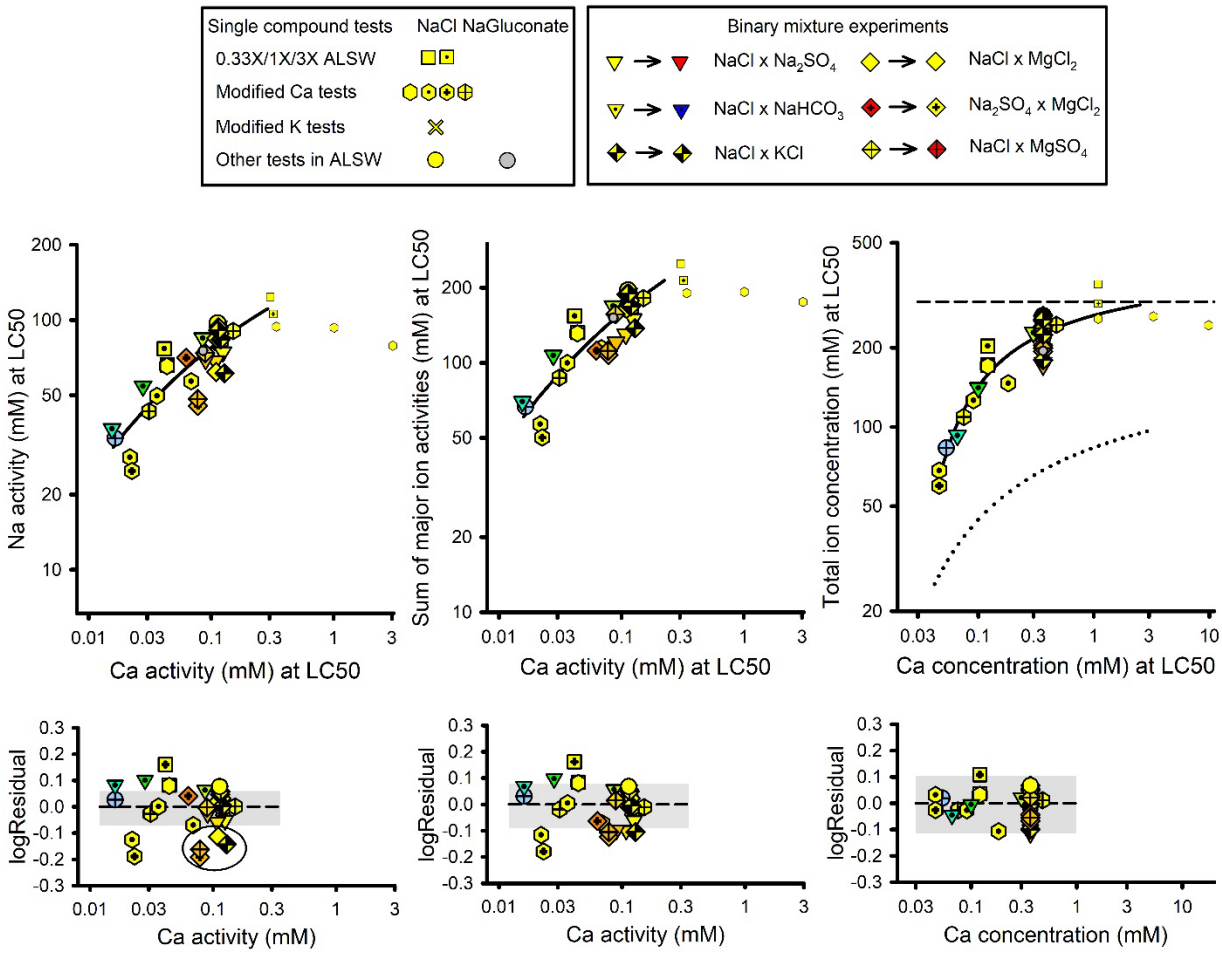
Single compound tests
NaCl NaGluconate
0.33X/1X/3X ALSW
Modified Ca tests
Modified K tests
Other tests in ALSW
Binary mixture experiments
NaCl x Na2SO4
NaCl x MgCl2
NaCl x NaHCO3
Na2SO4 x MgCl2
NaCl x KCl
NaCl x MgSO4
Na activity (mM) at LC50
Ca activity (mM) at LC50
Sum of major ion activities (mM) at LC50
Ca activity (mM) at LC50
Total ion concentration (mM) at LC50
Ca concentration (mM) at LC50
logResidual
Ca activity (mM)
logResidual
Ca activity (mM)
logResidual
Ca concentration (mM)